ISSN: 2831 - 6789

Research Article

Journal of Robotics and Automation Research

The calculation of the allowable diametrical inaccuracy of the cycloidal driving bores in a cycloidal drive with a given profile error and transmission ratio fluctuation

Attila Csobán

Department of Machine and Product Design Faculty of Mechanical Engineering Budapest University of Technology and Economics 1111, Műegyetem rkp. 3, Budapest, Hungary

***Corresponding author**
Attila Csoban, Department of Machine and Product Design Faculty of Mechanical Engineering Budapest University of Technology and Economics 1111, Műegyetem rkp. 3, Budapest, Hungary.

Submitted: 13 Oct 2022; **Accepted:** 19 Oct 2022; **Published:** 26 Nov 2022

Citation: *Attila Csoban. (2022). The calculation of the allowable diametrical inaccuracy of the cycloidal driving bores in a cycloidal drive with a given profile error and transmission ratio fluctuation. J Robot Auto Res, 3(3), 308-315.*

Abstract

Cycloidal drives are getting more and more widespread due to their beneficial properties. The greatest advantage of these transmissions compared to other general-purpose industrial transmissions, but even compared to the more widespread types of planetary gears, is their ability to operate with large transmission ratios and good efficiency under larger performance density. However, high manufacturing accuracy is essential in order to ensure the steady operation of the transmission from a dynamic perspective. A smaller amount of play and the minimal fluctuation of transmission ratios, which fundamentally define the kinematic properties of these high precision premium transmissions, can only be achieved by increasing the manufacturing accuracy, decreasing the magnitude of manufacturing errors and limiting the tolerance field.

The current research, in line with the findings of multiple parametric studies and as part of an ongoing development project, has focused on finding the allowable manufacturing accuracy of transmissions that are primarily manufactured by small scale or by one-off production, because in case of such developments the right pricing is a huge risk with respect to marketability, which is essentially defined by the required manufacturing accuracy. The current research discusses the effect of the cycloidal driving bores diametrical inaccuracy in a cycloidal disc, that was manufactured with wire electrical discharge machining and contains profile defects, on the fluctuation of the transmission ratio and on the transmission play.

Keywords: Transmission Ratio Fluctuation, Profile Error, Diametrical Inaccuracy

Figure 1: Cycloidal drive before the measurements

Highlights:

1. Based on the findings, it is possible to define the production accuracy level of the planetary gear being a core component in case of cycloidal drives in a way that the drive achieves the required kinematic features and the expected dynamics figures.
2. If a particular application field does not require the use of the most accurate drive which does not have any backlash, it can be prescribed in the planning phase to implement the most cost-effective production technology.
3. Based on the findings, rotation angle varies linearly depending on the diameter failures of the driving bore (Δd) while it is not so remarkable depending on the profile failures (d). The results are indicated depending on profile failures and the diameter failures of the driving bores.
4. The results are shown in this paper.

Introduction

The investigation of the manufacturing defects' effect on the kinematic properties was performed assuming different levels of manufacturing inaccuracy and tolerance fields on the various tooth geometries. The required minimum accuracy for a given tooth geometry, which guarantees a pre-defined maximal transmission ratio fluctuation, can be defined from the obtained results. In order to solve the geometrical equations that define the connection, numerical methods and a software specifically written for this task were used. The magnitude of manufacturing defects was defined based on given tolerance fields in order to define the kinematic properties.

The definition of the transmission ratio fluctuation, that was caused by manufacturing defects, was done numerically for different gear geometries and for different cycloidal driving bores. The results show that the transmission ratio changes as a function of the rotation angle of the drive shaft. Based on the maximum transmission ratio fluctuation for a given module, profile defect and number of teeth and by using a derived analytical approximation, the required manufacturing accuracy for the dimensions of the cycloidal driving bores can be predicted for a given maximum transmission ratio inaccuracy.

Production Failures

In the main components of drives with cycloidal crogs, diameter failures of the pitch-circle may occur, there can be distribution failures, profile failures, diameter failures of driving bores or hit failures of the rolling circle, but hit failures of the planetary gear are also possible due to an excentrity failure. Equations made to find out how profile failures affect transmission can be solved by applying numerical methods, in case of this research in a Scilab environment. Earlier, when the connection between profile failures and transmission fluctuation was examined, it could be proved that transmission is not constant and it varies around the figure without any failures. Furthermore, the curve depicting transmission change is not continous. The reason for that is that there is only one cog pair connection due to the failure and the connected cog pairs vary during the motion of the planetary gear. Where the curve is interrupted, the former cog pairs leave the connection and the motion will be determined by the following cog pair. Consequently, each section of the curve belongs to different cog pairs.

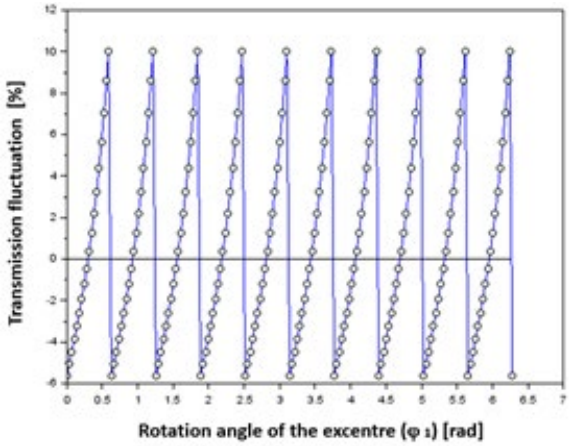

Figure 2: Transmissionfluctuation expressed in percentage

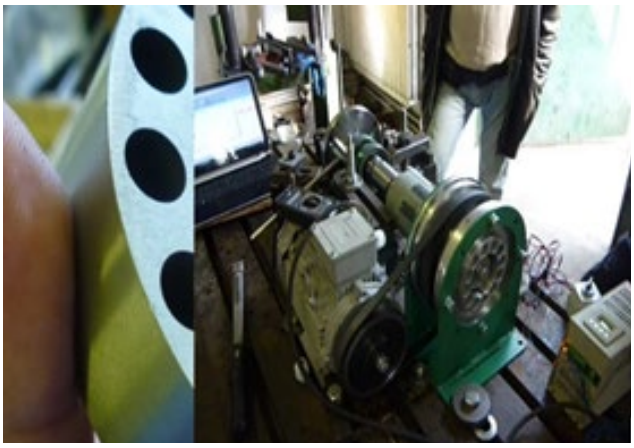

Figure 3: The connection between transmission fluctuation and profile failure is not only numerical, analytical, but it is also supported by measurements.

Consideration of Failures of Driving Boresoduction Failures

It has been proved by previous researches and measurements that backlash is developed by profile failure because the input shaft has to rotate so that a cog pair hits while the planetary gear is not rotating. In this chapter, backlash resulting from the diameter failure of driving bores (Δd) is also described in addition to the backlash generated by profile failures (figure 4).

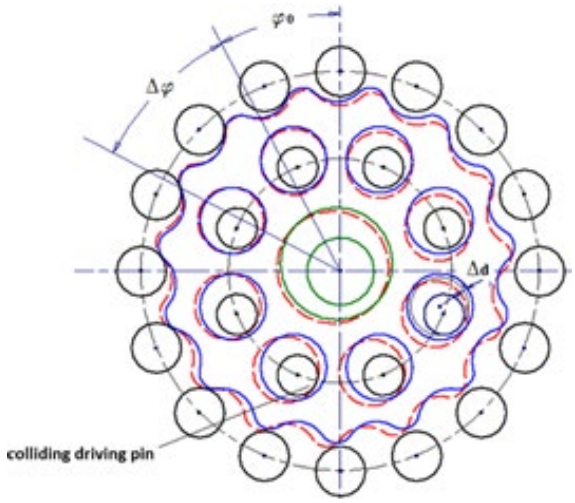

Figure 4: Backlashresultingfromthefailureof driving bores

In this figure, backlash resulting from profile failures are marked with φ_0 and backlash caused by a diameter failure of a driving bore is marked as Δf. After the input shaft rotates by φ_0, a cog pair will already be connected. After it keeps turning, the planetary gear will also rotate. In order to cause the output shaft to rotate as well, the driving pin has to hit (it is marked with an interrupted line in figure 4). The shaft rotation needed to enable this hit is marked as Δφ. In this chapter, the rotation angle Δφ is determined for a gear with different cog numbers. In case of both gears with the given cog numbers, the grade of the profile failure has been defined in advance determining the tolerance zone resulting from the diameter of the pitch-circle of the planetary gear and the particular accuracy level. Like in case of profile failures, driving bore failures have been estimated in due consideration of the tolerance zones applicable to the different accuracy levels.

Equations

In order to define the rotation angle needed for the hit of a driving pin, we can establish the geometrical equations according to the following figure:

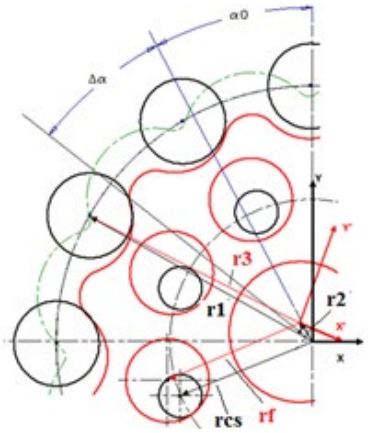

Figure 5: Applicable equations

According to the equation describing the connection of two cog pairs:

$$\mathbf{r}_1 = \mathbf{T} \cdot \mathbf{r}_{3(\varphi)} + \mathbf{r}_{2\,(\varphi 1)} \quad (1)$$

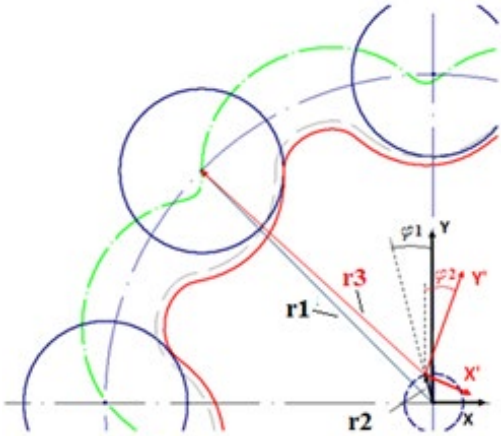

Figure 6: Determination of the rotation angle of the planetary gear

Besides, the following connection (equation) can be established when the driving bore and the driving pin come into contact:

$$|\mathbf{r}_2 + \mathbf{r}_f - \mathbf{r}_{cs}| = \boldsymbol{e} + \Delta d \quad (2)$$

where:

- $\mathbf{r}_1$ - is the vector pointing at the center of the connected pin,
- **T** - is the transformation matrix:

T=[cosφ$_2$&sinφ$_2$@-sinφ$_2$&cosφ$_2$]

- $r_{3(\varphi)}$ - is the vector containing the parameter equations describing the shifted curve in the coordinate system X'Y' where φ is the parameter of the equations describing the curve,
- r2 (φ1) - is the vector pointing at the center point of the planetary gear and f1 is the angle determining the location of the excenter,
- φ1 - is the rotation angle of the input shaft,
- φ2(φ1) - is the rotation angle of the planetary gear,
- $\mathbf{r}_f$ - is the vector pointing at the center of the driving bore,
- $\mathbf{r}_{cs}$ - is the vector pointing at the centerpoint of the colliding driving pin,
- *e* - excentrity (axial distance),
- Δ*d* - diameter failure of the driving bore.

After solving the above-mentioned equations, we receive the figures of $\varphi_1=\Delta\varphi,\varphi_2,\varphi$, where the driving pin hits. The process diagram of the algorhytm of the calculation:

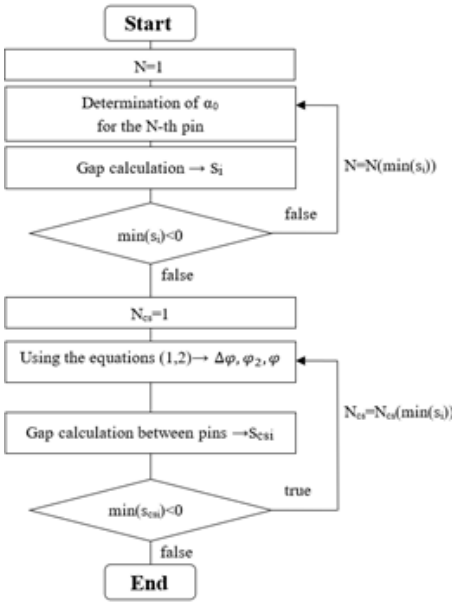

Figure 7: Block diagram of the algorhytm

Marks used in the block diagram:

- α - rotation angle of the excentre required for the collosion,
- N - number of the connected pins,
- N_{cs} - number of the driving pins,
- s_i - gap calculated at the pin i,
- s_{csi} - gap between the driving pin and the driving bore,
- N(min(si)) - number of pins defined for the minimum gap,
- Ncs(min(si)) - number of the driving pin with the smallest gap.
- φ_1 - rotation angle of the excenter, $\varphi_1=\varphi_0 \ldots \varphi_n$
- φ_2 - rotation angle of the planetary gear,
- $\Delta\varphi_1$ - grade of the rotation angle of the excenter.

Examined Geometries

Calculations have been performed for two gear geometries.

Table 1: Common parameters of the gears:

Module: (m)	3 [mm]
Addendum modification: (x)	0.25 [-]
Generating circle radius factor: (r_c^*)	1 [-]
Number of the driving pins: (N_{cs})	8 [-]
Diameter of the driving pins: (d_{cs})	20 [mm]
Diameter of the driving bores:(d_f)	22.25 [mm]
Bolt circle diameter of the driving bore and of the driving pins: (D)	80 [mm]

Gears differ from each other in terms of the cog number, for the first gear z1=43 [-] and for the other gear z1=50 (Figure 8).

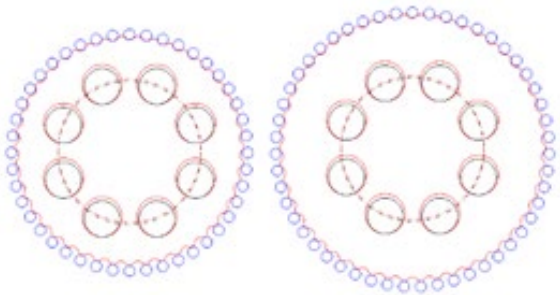

Figure 8: Gears with the following cog number: z1=43 and z1=50

The following chart shows the diameter of the pitch-circle of the gears dz43=126 and dz50=150, and the profile failures which are assigned to these figures.

Table 2: Profile failures belonging to a particular cog number:

	Profile Error				
	IT5	IT6	IT7	IT8	IT9
z1=43	0,05	0,0315	0,02	0,0125	0,009
z1=50	0,05	0,0315	0,02	0,0125	0,009

Diameter failures of the driving bores:

Table 3: Diameter error of driving bores

Diameter error of the driving bores				
IT5	IT6	IT7	IT8	IT9
0,0045	0,0065	0,0105	0,0165	0,026

Results

The Δφ rotation angle figures resulting from the calculation are summarized in the following charts. The findings are shown in the following diagrams. The results are indicated depending on profile failures and the diameter failures of the driving bores. A surface has been fitted to the points using the method of the smallest squares. It is also depicted.

Results in case of a cog number of z1=43:

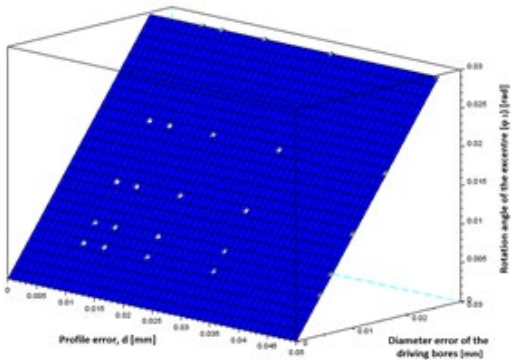

Figure 9: Rotation angle figures in case of z1=43

Equation applicable to the surface fitted to the points:

$$\Delta\varphi=1.1437\cdot\Delta d-7686\cdot10^{-4}\cdot\Delta d\cdot d \qquad (3)$$

where:

- Δd is the diameter error of the driving bore [mm],
- d is a profile error [mm].

Results in case of a cog number of z1=50:

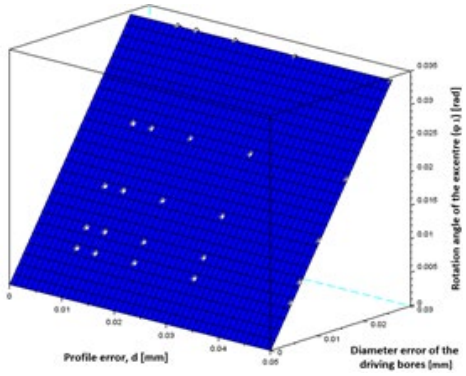

Figure 10: Rotation angle figures in case of z1=50

Equation applicable to the surface fitted to the points:

$$\Delta\varphi=1.3273\cdot\Delta d-8458\cdot10^{-4}\cdot\Delta d\cdot d \qquad (4)$$

Based on the findings, rotation angle varies linearly depending on the diameter failures of the driving bore (Δd) while it is not so remarkable depending on the profile failures (d).

Table 4: Geometrical dimensions of the gears

Parameter	Value				Dim.
Number of teeth planet-gear: (z1)	21	59	105	143	-
Number of teeth ring gear: (z2)	22	60	106	144	-
Gear ratio: (i)	21	59	105	143	-
Module: (m)	1.5	1.5	1.5	1.5	mm
Pin radius factor: (r_c*)	1	1	1	1	-
Pin radius: (r_c)	1.5	1.5	1.5	1.5	mm
Width: (b)	1.65	4.5	7.95	10.8	mm
Min. Addendum modification: (x), x_{min}	0.093	0.083	0.080	0.079	-
Min. Addendum modification: (x), x_{max}	0.49	0.49	0.49	0.49	-
Chosen Addendum modification (x)	0.3	0.3	0.3	0.3	-
Addendum modification (X)	0.225	0.225	0.225	0.225	mm
Total gear depth (h)	1.05	1.05	1.05	1.05	mm
Planet-gear pitch radius: (r_1)	15.75	44.25	78.75	107.25	mm

Ring-gear pitch radius: (r_2)	16.5	45	79.5	108	mm
Centre distance: (a_w)	0.525	0.525	0.525	0.525	mm
Planet-gear working pitch radius (r_{w1})	11.025	30.975	55.125	75.075	mm
Ring-gear working pitch radius (r_{w2})	11.55	31.5	55.65	75.6	mm
Driving pin diameter: (d)	4	11	20	30	mm

In the following charts, profile failures belonging to a planetary gear with a particular module and cog number are shown. Each chart relates to a particular module and profile failures belonging to different cog numbers (columns) are indicated according to different accuracy levels (rows).

Table 5: Profile failures in case of m=1 [mm].

	z1	9	25	43	53	117
IT	5	0.003	0.0045	0.0055	0.0065	0.0075
	6	0.0045	0.0065	0.008	0.0095	0.011
	7	0.0075	0.0105	0.0125	0.015	0.0175
	8	0.011	0.0165	0.0195	0.023	0.027
	9	0.018	0.026	0.031	0.037	0.0435

Table 6: Profile failures in case of m=2 [mm].

	z1	9	25	43	53	117
IT	5	0.004	0.0055	0.0075	0.0075	0.01
	6	0.0055	0.008	0.011	0.011	0.0145
	7	0.009	0.0125	0.0175	0.0175	0.023
	8	0.0135	0.0195	0.027	0.027	0.036
	9	0.0215	0.031	0.0435	0.0435	0.0575

Table 7: Profile failures in case of m=3 [mm].

	z1	9	25	43	53	117
IT	5	0.0045	0.0065	0.009	0.009	0.0125
	6	0.0065	0.0095	0.0125	0.0125	0.018
	7	0.0105	0.015	0.02	0.02	0.0285
	8	0.0165	0.023	0.0315	0.0315	0.0445
	9	0.026	0.037	0.05	0.05	0.07

Table 8: Profile failures in case of m=5 [mm].

	z1	9	25	43	53	117
IT	5	0.0055	0.009	0.01	0.0115	-
	6	0.008	0.0125	0.0145	0.016	-
	7	0.0125	0.02	0.023	0.026	-
	8	0.0195	0.0315	0.036	0.0405	-
	9	0.031	0.05	0.0575	0.065	-

In the following charts, transmission fluctuation values are shown (indicated in percentage) assigned to planetary gears with a particular module and cog number. Each chart relates to a particular module and fluctuation figures belonging to different cog numbers (columns) are indicated according to different accuracy levels (rows).

Table 9: Transmission fluctuation in case of m=1 [%].

	z1	9	25	43	53	117
IT	5	0.406642	0.175561	0.118517	0.112695	0.05738
	6	0.605794	0.251967	0.171999	0.163288	0.083349
	7	0.996186	0.401931	0.265262	0.253855	0.130306
	8	1.439023	0.620144	0.40575	0.380872	0.196182
	9	2.287451	0.950549	0.625551	0.591149	0.303765

Table 10: Transmission fluctuation in case of m=2 [%].

	z1	9	25	43	53	117
IT	5	0.272352	0.107898	0.08165	0.065543	0.038522
	6	0.373185	0.156307	0.119128	0.095636	0.055506
	7	0.605794	0.242469	0.187711	0.150721	0.087019
	8	0.899552	0.374095	0.285666	0.229428	0.133852
	9	1.407824	0.584313	0.449789	0.361376	0.207985

Table 11: Transmission fluctuation in case of m=3 [%].

	z1	9	25	43	53	117
IT	5	0.20474	0.085173	0.065468	0.052551	0.032177
	6	0.29482	0.124078	0.090609	0.072736	0.046096
	7	0.473327	0.194754	0.143898	0.115529	0.07228
	8	0.737077	0.296093	0.224108	0.179962	0.105883
	9	1.145266	0.469441	0.349534	0.280764	0.171124

Table 12: Transmission fluctuation in case of m=5 [%].

	z1	9	25	43	53	117
IT	5	0.150424	0.070844	0.043778	0.040373	-
	6	0.218288	0.098169	0.063305	0.056021	-
	7	0.339651	0.156307	0.099902	0.090499	-
	8	0.526458	0.24437	0.155164	0.139786	-
	9	0.828283	0.383388	0.236076	0.22124	-

The following two charts show backlash figures of the input shaft resulting from diameter failures of the driving bores and profile failures of the planetary gear. Columns of the charts belong to a particular driving bore failure while rows show the particular profile failures.

Table 13: Rotation angle [rad] figures belonging to the following cog number: z1=43

		Diameter error of the driving bores				
		0.0045	0.0065	0.0105	0.0165	0.026
Profile error	**0.009**	0.005207	0.007513	0.012112	0.018975	0.029765
	0.0125	0.005201	0.007505	0.012098	0.018955	0.029735
	0.02	0.005188	0.007487	0.01207	0.018913	0.029674
	0.0315	0.00517	0.007461	0.012029	0.018852	0.029585
	0.05	0.005143	0.007423	0.01197	0.018763	0.029456

Table 13: Rotation angle [rad] figures belonging to the following cog number: z1=50

		Diameter error of the driving bores				
		0.0045	0.0065	0.0105	0.0165	0.026
Profile error	**0.009**	0.006051	0.00873	0.01407	0.022035	0.034545
	0.0125	0.006044	0.00872	0.014053	0.02201	0.034508
	0.02	0.006028	0.008698	0.014019	0.021958	0.034433
	0.0315	0.006006	0.008665	0.013968	0.021883	0.034323
	0.05	0.005972	0.008618	0.013894	0.021772	0.034162

Conclusions

Based on the findings, it is possible to define the production accuracy level of the planetary gear being a core component in case of cycloidal drives in a way that the drive achieves the required kinematic features and the expected dynamics figures. If a particular application field does not require the use of the most accurate drive which does not have any backlash, it can be prescribed in the planning phase to implement the most cost-effective production technology.

Acknowledgements

The research reported in this paper and carried out at BME has been supported by the NRDI Fund (TKP2020 NC, Grant No. BME-NCS) based on the charter of bolster issued by the NRDI Office under the auspices of the Ministry for Innovation and Technology.

Hereby, I would like to express my thanks to the engineering student Mr. Dávid Roboz who made a considerable contribution to my research by doing a great job.

References

1. Chmurawa, M., & Lokiec, A. (2001, November). Distribution of loads in cycloidal planetary gear (CYCLO) including modification of equidistant. In 16th European ADAMS user conference, Berchtesgaden, Germany.
2. Thube, S. V., & Bobak, T. R. (2012). Dynamic analysis of a cycloidal gearbox using finite element method. AGMA Technical Paper, 1-13.
3. Kumar, N. (2015). Investigation of drive-train dynamics of mechanical transmissions incorporating cycloidal drives (Doctoral dissertation, Queensland University of Technology).
4. Borislavov, B., Borisov, I., & Panchev, V. (2012). Design of a planetary-cyclo-drive speed reducer: cycloid stage, geometry, element analyses.
5. Cyclo Drive 6000 Gearmotors & Speed Reducers. (2016).
6. Fine Cyclo Zero Backlash Speed Reducers. (2016).
7. Comparison of Circulate 3000 & the SM-Cyclo Speed Reducers. (2016).
8. Precision Reduction Gear RV. (2016).
9. Zero Backlash Speed Reducer. (2016).
10. Roladrive Speed Reducer. (2016).
11. Tsai, S. J., Huang, C. H., Yeh, H. Y., & Huang, W. J. (2015, October). Loaded tooth contact analysis of cycloid planetary gear drives. In Proceedings of the 14th IFToMM World Congress (pp. 227-234).
12. Yang, D. C. H., & Blanche, J. G. (1990). Design and application guidelines for cycloid drives with machining tolerances. Mechanism and Machine Theory, 25(5), 487-501.